

Limits on coupling between dark components

Roberto Mainini, Silvio Bonometto

Department of Physics G. Occhialini – Milano–Bicocca University, Piazza della Scienza 3, 20126 Milano, Italy & I.N.F.N., Sezione di Milano

Abstract. We debate the observational effects of DM–DE coupling and outline that, in the case of a ϕ dependent coupling, the shape of the transfer function can be significantly modified, because of the suppression of Meszaros’ effect, between the entry of a scale in the particle horizon and matter–radiation equality. Therefore, a fair deal of models with an evolving coupling conflicts with data, unless the suppression is balanced by a shift of the primeval spectral index, in the suitable scale range.

PACS numbers: 98.80.-k, 98.65.-r

1. Introduction

There can be little doubts that a tenable cosmological model must include at least two dark components, cold Dark Matter (DM) and Dark Energy (DE); yet only hypotheses on their nature exist, most of them assuming that DM and DE are physically unrelated and that their similar densities, in today's world and just in it, are purely accidental.

Attempts to overcome this conceptual deadlock were made by several authors suggesting, first of all, that DE has a dynamical nature [1] (for a review see [2] and references therein). An alternative idea is that DE is a phenomenological consequence of the emergence of nonlinearity; this appealing option was repeatedly considered (see, e.g., [3] and references therein), but is far from being shown and leaves however apart the question of DM nature. Interactions between DM and dynamical DE [4] (see also [5]) might partially cure the problem, keeping close values for their densities up to large redshift. This option could also be read as an approach to a deeper reality, whose physical features could emerge from phenomenological limits to coupling strength and shape.

A longer step forward was attempted by [6], suggesting that DM and DE derive from a single complex scalar field, being its quantized phase and modulus, respectively. The complex field could be the one responsible for \mathcal{CP} conservation in strong interactions, within a scheme similar to Peccei & Quinn framework [7] (see also [8]). At variance from previous suggestions, which introduce parameters and aim at limiting them through data fitting, this option – dubbed *dual-axion* model – cuts the available degrees of freedom, including as many parameters as a standard-CDM approach. It is then quite appealing that its reduced parameter budget is sufficient to fit quite a number of observational constraints [9], still allowing for a common nature of DM and DE and for a specific shape of interaction between them.

In this paper, however, we keep on the phenomenological side and discuss generic constraints to DM-DE interactions. This discussion will have a fallout also on the *dual-axion* approach, which does face a problem, because of the feature of the DM-DE coupling it causes.

A coupling of baryons with DE is ruled out by observational consequences similar to modifying gravity. Limits are looser for DM-DE coupling, whose consequences can be appreciated only over cosmological distances. It should also be outlined that forces acting within the dark sector could modify predictions on high concentration DM lumps. There can be little doubts that cold DM particles, feeling gravity only, give them NFW profiles. Yet, observational data do not lend much support to this shape, for any scale range, and direct interaction between DM particles is severely constrained also by recent data.

This is a further reason to consider DM-DE interactions, either as a fundamental theory or as an effective framework to approach deeper physics. It is then important to devise any observational limit to such interactions and, in this paper, we outline further constraints to its shape; they are consequences of the early behavior of density

fluctuations, over scales destined to evolve into non-linear structures.

Fluctuations over such scales enter the horizon before matter-radiation equality and their growth is initially inhibited by the overwhelming density of the radiative component, then still behaving as a single fluid together with baryons. While fluctuations in the fluid behave as sonic waves, self gravitation of DM is just a minor dynamical effect in respect to cosmic expansion. This freezing of fluctuation amplitudes until equality is known as *Meszaros effect*.

The main point we wish to outline here is that DM-DE coupling can damp Meszaros effect, so that the rate of fluctuation growth, between the entry in the horizon and equality, is significantly enhanced.

As a matter of fact, fluctuation freezing is essential, in shaping the transferred spectrum, which peaks on the scale k_{eq} entering the horizon at equality. At smaller mass scales ($k > k_{eq}$) the spectrum declines because of the increasing duration of the freeze.

In the presence of a significant DM-DE coupling the whole scenario can suffer substantial modifications. Discussing them is the aim of this technical paper. We warn the reader that no general data fitting, constraining parameters and/or showing specific model advantages, will be made here. This is why we keep to cosmological parameter values ensuing from WMAP3 best-fit [10], although deduced by assuming a Λ CDM model. In particular, we shall take an overall density parameter $\Omega = 1$; the present value of the cold DM (baryon) density parameter will be $\Omega_{o,c} = 0.224$ ($\Omega_{o,b} = 0.044$); the dimensionless Hubble parameter will be $h = 0.704$; the primeval spectral index, when not taken as a free parameter, will be $n = 0.947$.

Within this frame we shall consider a self-interacting scalar field, causing cosmic acceleration when its pressure/density ratio $w = p_{DE}/\rho_{DE}$ falls in the range $(-1, -1/3)$. Quite in general, it is

$$\rho_{DE} = \rho_{k,DE} + \rho_{p,DE} \equiv \dot{\phi}^2/2a^2 + V(\phi), \quad p_{DE} = \rho_{k,DE} - \rho_{p,DE}, \quad (1)$$

so that it is $-1/3 \gg w > -1$ when dynamical equations yield $\rho_{k,DE}/V \ll 1/2$. Here

$$ds^2 = g_{\mu\nu}dx^\mu dx^\nu = a^2(\tau)(-d\tau^2 + dx_i dx^i) \quad (i = 1, \dots, 3) \quad (2)$$

is the background metric and dots indicate differentiation with respect to τ (conformal time). The w ratio exhibits a time dependence set by the shape of $V(\phi)$. Much work has been done on dynamical DE (see, e.g., [2] and references therein), also aiming at restricting the range of acceptable $w(\tau)$'s, so gaining an observational insight onto the physics responsible for the potential $V(\phi)$.

Our analysis here will however be restricted to SUGRA potentials [11]

$$V(\phi) = (\Lambda^{\alpha+4}/\phi^\alpha) \exp(4\pi\phi^2/m_p^2) \quad (3)$$

admitting tracker solutions. This will enable us to focus on peculiarities caused by the coupling. Let us also remind that, once the DE density parameters Ω_{DE} is assigned, either α or the energy scale Λ , in the potentials (3), can still be freely chosen. In this paper we show results for $\Lambda = 10^2$ GeV.

The SUGRA potential, at least in the absence of coupling, yields an excellent fit of observational data [12]. We tested the effects of coupling for a number of values of the scale Λ , from 10 to 10^4 , and also changing the shape of the potential into Ratra–Peebles.

In the former case we find just marginal shifts. In the latter one, quantitative changes can be significant. The overall behavior is however identical and this potential is known to yield a poor fit to CMB data, unless quite a small Λ scale is taken, so spoiling its physical appeal.

Within this frame we aim at focusing problems and showing the quantitative consequences of different options. In the next section we focus soon on the reason causing the suppression of Meszaros effect. In Section 3 we deepen the analytical treatment. In Section 4 we present our results through a number of plots. Section 5 is then devoted to a final discussion.

2. Overcoming the freeze

In the next section we shall report the equations followed by fluctuations, in the presence of DM–DE coupling. It is however worth focusing soon on the critical point, where the coupling strength competes with Meszaros’ freezing.

On a scale below the horizon and on a time before matter–radiation equality, the equation obeyed by DM fluctuations essentially reads

$$\ddot{\delta}_c + \left[\frac{\dot{a}}{a} - \frac{4}{m_p} \sqrt{\frac{\pi}{3}} \tilde{\beta}(\phi) \dot{\phi} \right] \dot{\delta}_c - 4\pi G a^2 \rho \left\{ \left[1 + \frac{4}{3} \tilde{\beta}^2(\phi) \right] \Omega_c \delta_c + \Omega_{\gamma b} \delta_{\gamma b} [1 + 3c_s^2] \right\} = 0, \quad (4)$$

as we shall show in detail in the next section. Here, as usual, a is the scale factor; ρ is the overall density; Ω_c and $\Omega_{\gamma b}$ are time dependent density parameters for DM and the baryon–photon fluid; $m_p = G^{-1/2}$ is the Planck mass. The relevant physics, instead, is carried by: (i) $\tilde{\beta}(\phi)$, gauging the coupling strength which, in general, is a function of the very field ϕ ; (ii) the speed of sound

$$c_s^2 \equiv \delta p_\gamma / (\delta \rho_b + \delta \rho_\gamma) = [3(1 + 3\Omega_b/4\Omega_\gamma)]^{-1} \quad (5)$$

and also the state parameter

$$w_{\gamma b}(a) \equiv p_\gamma / (\rho_b + \rho_\gamma) = [3(1 + \Omega_b/\Omega_\gamma)]^{-1} \quad (6)$$

of the baryon–photon fluid. In fact, eq. (4) essentially coincides with the customary equation in the absence of coupling, if we drop the $\tilde{\beta}$ terms. It should be also outlined that, here, neutrino fluctuation effects are disregarded.

Let us then outline first that, in average, the term $\Omega_{\gamma b} \delta_{\gamma b} (1 + 3c_s^2)$ almost vanishes, as sonic waves fluctuate. Then, in the absence of coupling ($\tilde{\beta} = 0$), the self–gravitation term $\propto \delta_c$ is also damped by $\Omega_c \ll 1$. If the photon–baryon term is then neglected, the increasing mode obtainable from the resulting equation (approximately) reads

$$\delta_c \propto 1 + 3y/2 \quad (7)$$

with $y = 3w_{\gamma b} a/a_{eq}$ (see, e.g., [13]) and this yields a growth from horizon to equality never exceeding a factor 2.5, that we shall approximate as $\delta_c \propto a^{1/4}$, according to

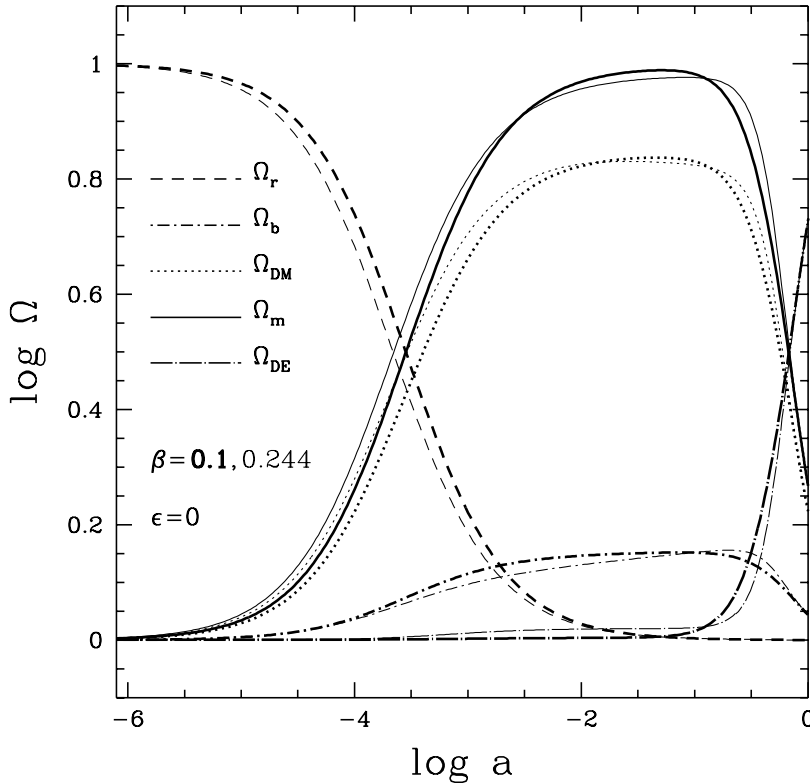


Figure 1. Scale dependence of the density parameters of the various components in coupled DE models with constant coupling. This plot shows also the displacement of z_{eq} and, henceforth, of k_{eq} as β increases: thicker (thinner) curves refer to $\beta = 0.01$ (0.0244).

numerical outputs. Meanwhile, above the horizon, in a synchronous gauge, $\delta_c \propto a^2$. Hence, for $k > k_{eq}$, the growth is slowed down by a factor $\propto a_h^{7/4}(k)$, while the scale factor when k passes through the horizon, $a_h(k) \propto k^{-1}$. Altogether, for $k > k_{eq}$, we expect a transferred spectrum $P(k) = A k^n \mathcal{T}^2(k) \simeq A k^{n-3.5}$ ($\mathcal{T}(k)$ is the transfer function).

It is then easy to see what can change because of the coupling. The coefficient of the *friction term* $\propto \dot{\delta}_c$ is certainly reduced and can even invert its sign. Even more significantly, the term $[1 + 4\tilde{\beta}^2(\phi)/3]\Omega_c$ can attain or overcome unity, not only because of the greater size of $\tilde{\beta}(\phi)$, but also thanks to the modified time dependence of Ω_c . It turns out, in fact, that an decreasing dependence of $\tilde{\beta}$ on ϕ yields higher Ω_c values in the relevant redshift interval. Quite in general we shall set

$$\tilde{\beta}(\phi) = \beta(\phi/m_p)^\epsilon \quad (8)$$

and argue that this assumption covers most significant cases. A decreasing dependence means then that $\epsilon < 0$. We can expect ϕ to be smaller at earlier times and to approach m_p toward the present epoch. Then, $\epsilon < 0$ causes a stronger coupling in the past.

Let us however debate first the constant coupling case ($\epsilon = 0$). Available data set then a constraint $\beta < 0.1$ – 0.2 [14] (see also [15]; beware of the different coupling definition), limiting the acceptable discrepancy of DM and DE evolution, after

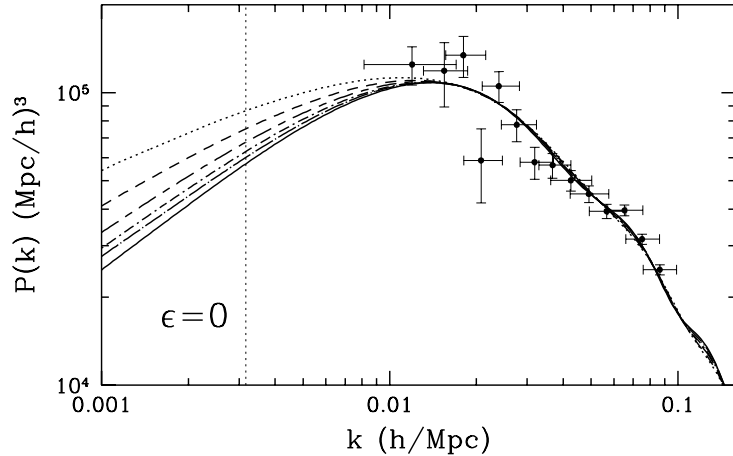


Figure 2. Best fits of SLOAN data for constant β from 0 (solid line) to 0.25 (dotted line). Different lines correspond to a β increase by 0.05. The vertical dotted line yields the scale of C_{10} .

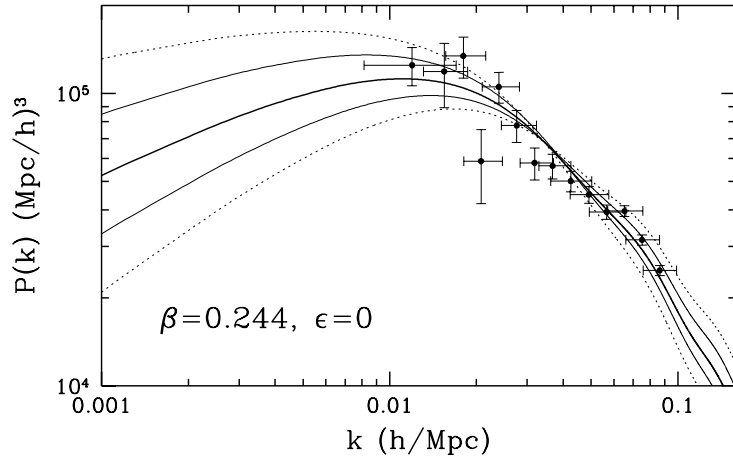


Figure 3. If values of n at 1- or 2- σ 's from best fits are taken, spectra are significantly modified. Here we show the effect in the case with $C = 1/m_p$.

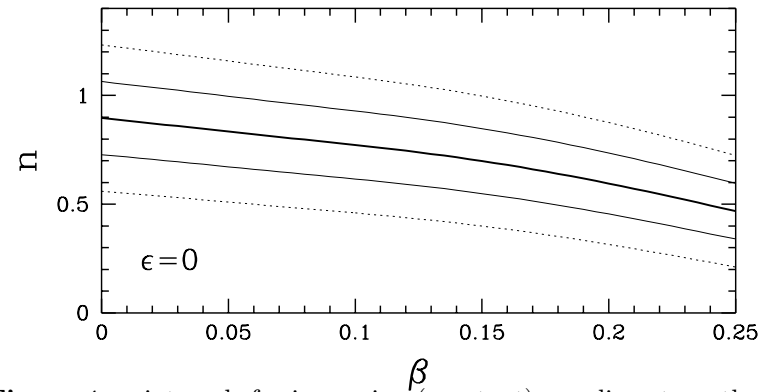


Figure 4. n intervals for increasing (constant) coupling strength

recombination, from uncoupled models. The most direct effect, in this case, concerns large scales entering the horizon late, when such discrepancies occur. The low- ℓ plateau of the CMB anisotropy spectrum can then undergo a modified ISW effect, while some changes in the C_ℓ behavior, up to the first peak at $\ell \sim 200$, can be compensated by slightly modifying n , h and other parameters.

Even more significant shifts occur on the transfer function. Its slope, at $k > k_{eq}$ and up to a scale $k \sim 0.1/h\text{Mpc}^{-1}$, where non-linearity effects become important, is slightly distorted as β increases. The main effect, however, is a progressive displacement of k_{eq} itself. In Figure 1 we compare the Ω evolution in models with different constant coupling, showing the significant displacement of the crossing between Ω_r and Ω_c , when different β 's are taken.

We can show the impact of this displacement by fitting transferred spectra, over these scales, with the Luminous Red Galaxies sample data from the Sloan Digital Sky Survey (SDSS) [16] and allowing the primeval spectral index n , assumed to be constant, to act as a free parameter.

In Figure 2 we show the result of this fit. Transferred spectra, when k_{eq} vary, easily accommodate deep sample data in the linear range, as the k_{eq} shift is compensated by a slightly smoother slope. All that however requires a non negligible decrease of n , and transferred spectra risk to become too high in the region where they should fit CMB data (the scale of the 10-pole is indicated in the Figure).

An attempt to balance this spectral distortion can be made by varying other parameters. It is then significant to consider Figure 3, showing deep sample data vs. transferred spectra computed with n 's within 1- and 2- σ 's from the best-fit. In the Figure we took $\beta = \sqrt{3/\pi}/4 \simeq 0.244$, a value bearing a peculiar significance, as better explained in the next Section.

Accordingly, in Figure 4, we show the 1- and 2- σ range of n , for constant coupling strength. Previous likelihood analysis showed that models with constant $\beta < \sim 0.2$ do not exhibit severe disagreements with data. Accordingly, we can consider viable those models which, at the 1- σ level, admit $n > \sim 0.75$. With reference to this admittedly qualitative criterion, we shall now consider the variable coupling case.

First of all, when coupling varies, the evolution of the density parameters exhibits significant discrepancies from the constant coupling behavior. The point is that, at high redshift, they further strengthen DM self-gravity, coherently with higher $\tilde{\beta}$ effects. Results of a numerical integrations, illustrating this issue, are shown in Figure 5, where we compare the redshift dependence of density parameters in constant ($\epsilon = 0$) and strongly variable ($\epsilon = -1$) coupling models, allowing to appreciate a substantial enhancement of Ω_c at the eve of equality. Altogether $[1 + 4\tilde{\beta}^2(\phi)/3]\Omega_c$ is significantly greater, and the freeze of δ_c , between horizon entry and equality, is almost canceled.

This explains the behaviors shown in Figure 6, which exhibit one of the main findings of this work. These plots are obtained from a numerical evaluations of δ_c , in models with different β for $\epsilon = 0$ or -1. In the former case, the high- z effect of coupling is marginal. In the latter one, the fluctuation growth is substantially enhanced, more

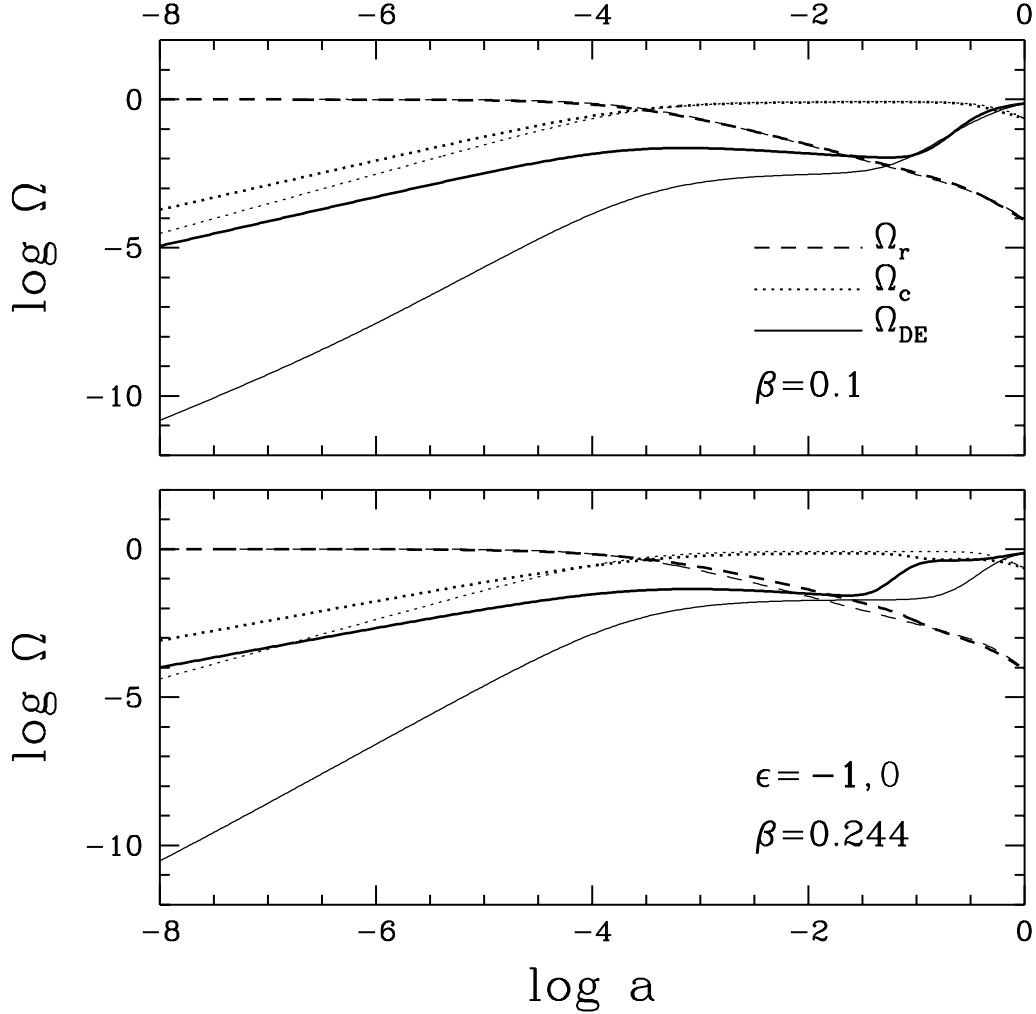


Figure 5. Redshift dependence of density parameters Ω in coupled DE models with constant and variable coupling. The two panels refer to different values of β . In both panels we show Ω 's for $\epsilon = 0$ ($C \propto \beta/m_p$, thinner lines) and $\epsilon = -1$ ($C \propto \beta/\phi$, thicker lines). Figures are rather intricate and their reading may begin from dashed lines, yielding $\Omega_r = \Omega_\gamma + \Omega_\nu$, which are almost independent from the coupling law. A more relevant effect occurs on Ω_c (dotted lines), whose values, in the case of variable coupling, exceed those of constant coupling until equality. The most relevant effect occurs for DE (solid lines), whose contribution to the overall density is enhanced by several order of magnitude by variable coupling. DE fluctuations will fade after the entry in the horizon; however, high Ω_{DE} values increase their impact on other components before their disappearance.

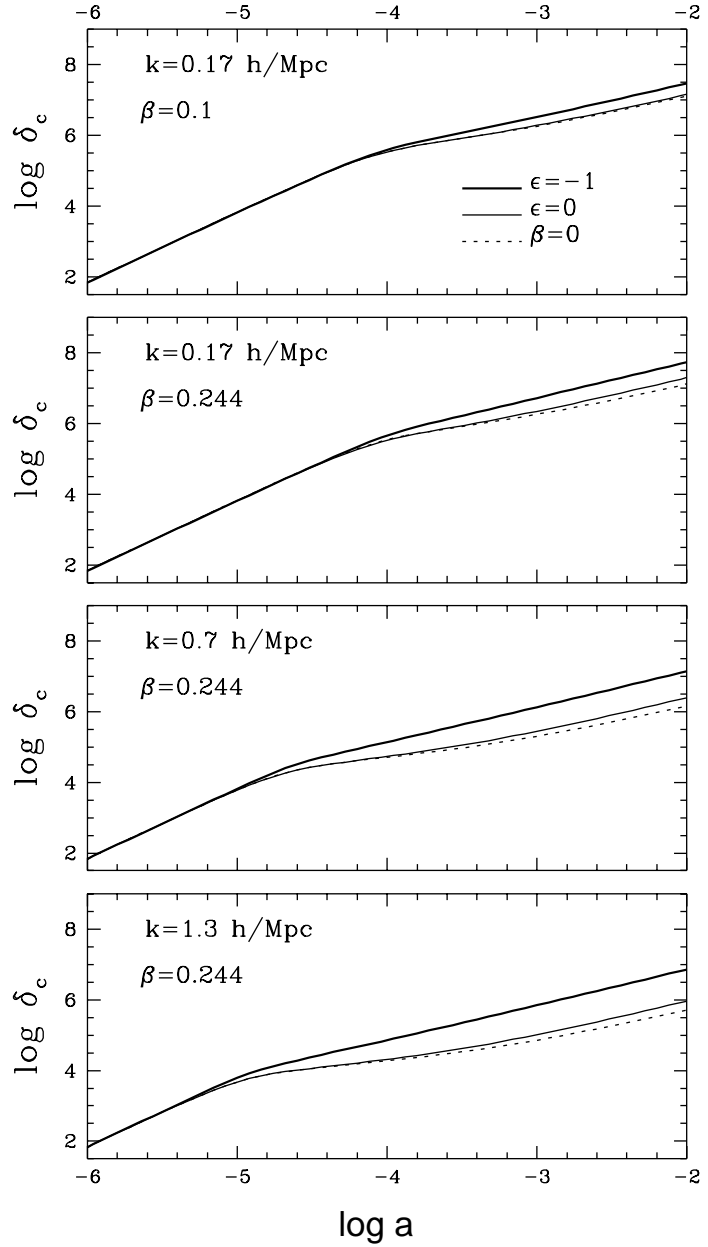


Figure 6. Evolution of DM fluctuations in a time interval enclosing the entry in the horizon and the matter–radiation equality. In all cases, in the presence of DM–DE coupling some modification occurs. They are however almost negligible for constant coupling, while, for coupling $\propto \phi^{-1}$, Meszaros’ freezing is almost completely canceled.

significantly for greater k values.

Accordingly, we can expect modifications in the transfer function and in the fit of observational data. Our general conclusion is that a time dependence of DM–DE coupling, making it stronger at higher redshift, can prevent DM fluctuations to have a stationarity period after their entry in the particle horizon, so causing large modification of the transfer function.

3. Dynamical equations

Using the metric (2), the background equations for DE and DM read

$$\ddot{\phi} + 2\frac{\dot{a}}{a}\dot{\phi} + a^2 V_{,\phi} = C(\phi)a^2 \rho_c, \quad \dot{\rho}_c + 3\frac{\dot{a}}{a}\rho_c = -C(\phi)\dot{\phi}\rho_c \quad (9)$$

where we set

$$C(\phi) = 4\sqrt{\frac{\pi}{3}} \frac{\beta}{m_p} \left(\frac{\phi}{m_p}\right)^\epsilon \quad (10)$$

A possible time dependence of the coupling strength was considered but not deepened since the early work of [17]. The *dual-axion* model naturally predicts a coupling $C = 1/\phi$, consistent with eq. (10), if $\epsilon = -1$ and $\beta \simeq 0.244$. Quite in general, for dimensional reasons, C can be expressed through products of m_p^a and ϕ^b with $a+b = -1$. During most cosmic evolution ϕ is a monotonically increasing function, so that the sign of the exponent of ϕ tells us whether the coupling was stronger or weaker in the past. (An exception can be recent times, as the exponential term in the SUGRA potential can cause a re-bounce of ϕ when it approaches m_p ; our arguments here concern much earlier times, when it is safely $\phi < m_p$).

An expression of C , made by a polynomial including terms with different powers of ϕ , could select a peculiar epoch to have then a weaker or stronger coupling. Such an option, however, is clearly *ad-hoc* and does not seem to deserve further investigation.

Instead of having the functional expression (10), of course, C could depend explicitly upon time. However, this would be hard to reconcile with the Lorentz invariance of the Lagrangian mass term

$$\mathcal{L}_c = -B(\phi)m_\chi\bar{\chi}\chi \quad (11)$$

setting the coupling between the DE scalar field ϕ and a spinor field χ supposed to yield DM, as $C(\phi) = d(\ln B)/d\phi$. (Notice that $B(\phi)m_\chi$ is the time-dependent mass of DM quanta.) A dependence of C on ϕ seems therefore the only pattern through which the coupling is allowed to depend on the cosmological time, without violating Lorentz invariance.

The DM–DE coupling affects also perturbation equations. In the relevant period, DM, photons and baryons can be treated as fluids; (massless) neutrinos, instead, are not a fluid. Fluctuations in a generic fluid with $p/\rho = w$ and $\delta p/\delta\rho = c_s^2$ fulfill the equations

$$\dot{\delta} = -(1+w)(kv + \dot{h}/2) - 3(c_s^2 - w)(\mathcal{H} - C\dot{\phi})\delta - (1-3w)(C\dot{\varphi} + C'\dot{\phi}\varphi)$$

$$\dot{v} = -(1-3w)(\mathcal{H} - C\dot{\phi})v + \frac{c_s^2}{1+w}k\delta - \frac{\dot{w}}{1+w}v - k\sigma - kC\frac{1-3w}{1+w}\varphi. \quad (12)$$

Here $\delta = \delta\rho/\rho$, $v = iu_ik^i/k$, $(\rho + p)\sigma = -(\hat{k}_i \cdot \hat{k}_j - \delta_{ij})(T^{ij} - \delta_{ij}T^k_k/3)$ (u_i are the space components of the velocity field in the fluid and T^{ij} is its stress-energy tensor) while the DE fields

$$\phi(\tau, \mathbf{x}) = \phi_o(\tau) + \varphi(\tau, \mathbf{x}) \quad (13)$$

is split into a background component ϕ_o , coinciding with the ϕ field obeying the eq. (9), and the space-dependent fluctuation φ ; in eqs. (12), Fourier components of φ are taken.

Eqs. (12) yield the DM equations for $w = 0$. In the case $\beta = 0$, without loss of precision, $v = 0$ can then be taken, so reducing them to one; however, this is no longer true when DM particles can be pushed by DE forces. Still from eqs. (12), we can also work out the equations for the photon-baryon fluid, by taking $C = 0$ and $w = w_{\gamma b}$ (eq. 6). The baryon component can be responsible for a shift of $w_{\gamma b}$ from $1/3$; although initially small, it can approach 20–25 % at the eve of recombination. Notice then that a non-vanishing factor $1 - 3w \sim \Omega_b/\Omega_\gamma$ keeps a direct influence of φ on baryon-photon fluctuations.

The equation fulfilled by φ then reads

$$\ddot{\varphi} + 2\mathcal{H}\dot{\varphi} + k^2\varphi + a^2V_\phi''\varphi + \dot{\phi}h/2 = Ca^2\rho_c\delta_c + C'_\phi a^2\rho_c\varphi, \quad (14)$$

while fluctuation self-gravity is fully accounted by \dot{h} , obtained by integrating the equation

$$\ddot{h} + \mathcal{H}\dot{h} = -8\pi G \left\{ a^2\rho[\Omega_{\gamma b}(1 + 3c_s^2)\delta_{\gamma b} + \Omega_c\delta_c] - 2a^2V_\phi'\varphi + \dot{\phi}\dot{\varphi} \right\} \quad (15)$$

This set of equations enables the reader to build a simplified numerical algorithm, directly testing the suppression of Meszaros' effect.

From eq. (12), eq. (4) is also obtainable. To show this, let us consider again eq. (14). There, any mass-like term multiplying ϕ , in comparison with k^2 , is negligible; then, before equality, it yields

$$\dot{\varphi} + (2/\tau)\dot{\varphi} + k^2\varphi = Ca^2\rho_c\delta_c - \dot{\phi}h/2 \quad (16)$$

Here, two kinds of time dependence must be compared, over fluctuation and Hubble time scales. Accordingly, we can express φ as sum of rapidly and slowly varying terms by actually summing up the (rapidly varying) general integral of the equation obtainable by equating to zero the l.h.s. and a (slowly varying) integral obtained by equating the last term at the l.h.s. with the r.h.s.. If we then time-average over fluctuation time scales, only the latter contribution survives and

$$\langle \varphi \rangle \simeq \frac{1}{k^2} (Ca^2\rho_c\delta_c - \dot{\phi}h/2) \quad (17)$$

Let us recall that dropping the contribution of fluctuating terms is the standard procedure to obtain an analytical description of Meszaros' effect. The point here is that, while all φ derivatives can be dropped, there is a slowly varying contribution to φ which cannot be soon disregarded.

However, if the expression (17) is used to replace φ in eqs. (12) for CDM, yielding

$$\dot{\delta}_c + kv_c + \frac{\dot{h}}{2} = -2\beta^2 \frac{d}{d\tau} \left[\left(\frac{\phi}{m_p} \right)^{2\epsilon} \frac{\Omega_c \delta_c}{(k\tau)^2} \right] + 4\sqrt{\frac{\pi}{3}} \frac{\beta}{k^2} \frac{d}{d\tau} \left(\frac{\dot{\phi} \dot{h}}{\phi^{-\epsilon} m_p^{1+\epsilon}} \right) \quad (18)$$

it becomes clear that also the slowly varying φ contributions can be dropped. In fact, the first term at the r.h.s. contains a division by $(k\tau)^2$, which is the squared ratio between long and short timescales and, altogether, it is $\sim \mathcal{O}[\dot{\delta}/(k\tau)^2] \ll \dot{\delta}$. We must then acknowledge that a time derivative of a quantity Q , varying over the Hubble time scale, is $\sim \mathcal{O}(Q/\tau)$. The second term at the r.h.s. is then $\sim \mathcal{O}[(\phi/m_p)^{1+\epsilon} \dot{h}/(k\tau)^2]$, while we took $1+\epsilon > 0$ and, in the epoch considered, $\phi/m_p \ll 1$. It must then be even smaller than the the first one.

Setting then to zero the l.h.s. of eq. (18), we obtain the relations

$$\ddot{\delta}_c + k\dot{v}_c + \frac{\ddot{h}}{2} \simeq 0, \quad kv_c \simeq -\dot{\delta}_c - \frac{\dot{h}}{2}. \quad (19)$$

In turn, the second eq. (12), using this latter equality, yields the relation

$$k\dot{v}_v = (C\dot{\phi} - \mathcal{H}) \left[-\dot{\delta}_c - \dot{h}/2 \right] - k^2 C \varphi, \quad (20)$$

which can be replaced in the former eq. (19), together with eq. (15) and (17), obtaining

$$\ddot{\delta}_c + [\mathcal{H} - C\dot{\phi}] \dot{\delta}_c - 4\pi G \left\{ a^2 \rho [\Omega_{\gamma b} (1 + 3c_s^2) \delta_{\gamma b} + \Omega_c \delta_c] - 2a^2 V'_\phi \varphi + \dot{\phi} \dot{\varphi} \right\} - C^2 a^2 \rho_c \delta_c = 0$$

Neglecting here φ fluctuations as source terms – DE yields a minor contribution to the overall density, as shown in Fig. 5 – and using eqs. (8) and (10), eq. (4) is soon obtainable. These arguments are fully confirmed if eqs. (12), (14), (15) are solved numerically.

4. Results

Otherwise, we can use the full set of equations and work out the transfer functions for matter fluctuations, by utilizing extensions of public programs like CAMB, or our own code, with identical outputs. They are shown in Fig. 7 for $\beta = 0.1$ and 0.244 , and a variety of values of ϵ .

The suppression of fluctuation freezing is obviously stronger for greater β (and increasingly negative ϵ values). For $\epsilon = -1$, enclosing the case $C = 1/\phi$ when $\beta = 0.244$, the steepness of the transfer function, for $k > k_{eq}$ is much reduced. The effect is still significant also for $\epsilon = -0.5$, namely when $\beta = 0.244$.

A further effect shown by these plots is a significant displacement of the scale where \mathcal{T} begins its gradual descent. As a consequence, different coupling laws may cause displacements on the scale where transferred spectra peak.

Figure 7 is a direct evidence that, in order to recover a fair slope of the transferred spectrum in the scale range where structures accumulate, smaller primeval n values are unavoidably required. In order to perform an evaluation of the effect, we actually built transferred spectra and compared them again with SLOAN data.

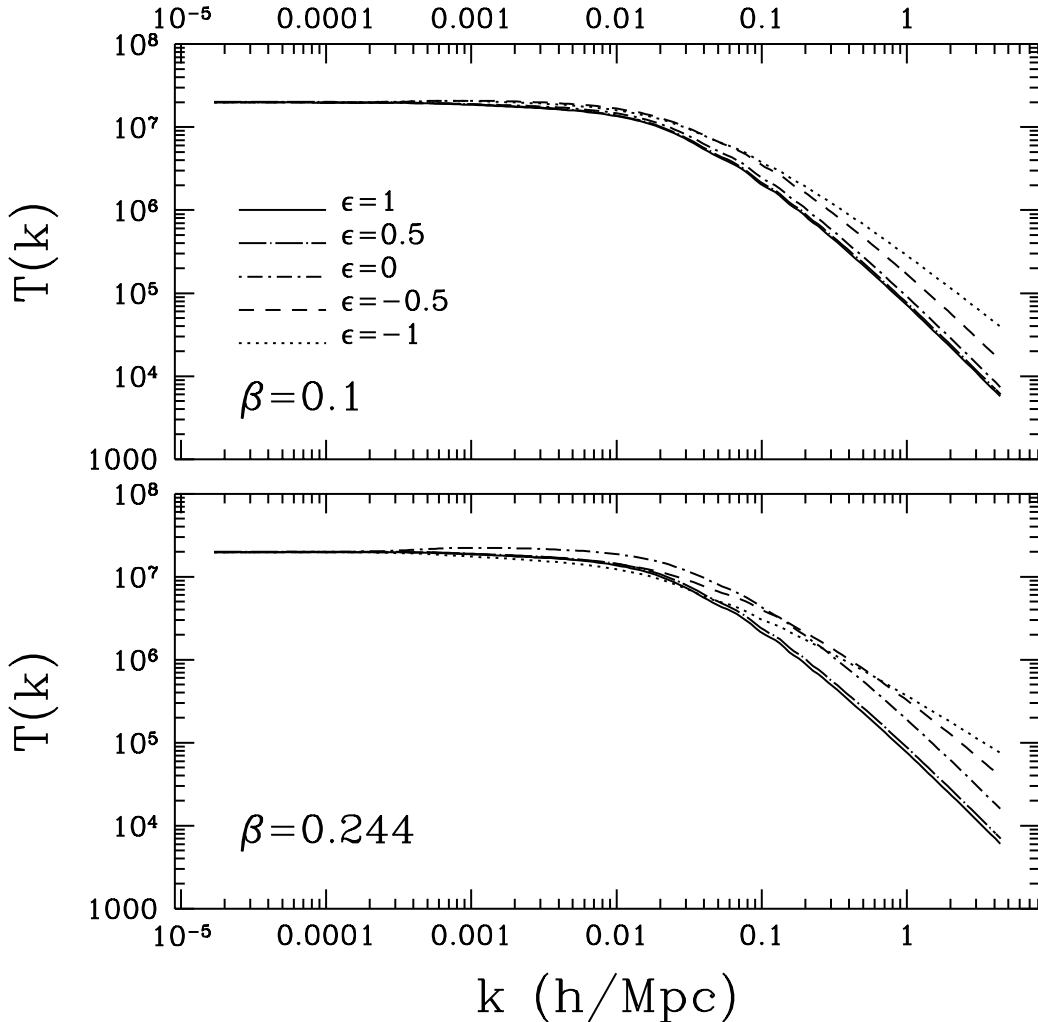


Figure 7. Transfer functions for different behaviors of DM-DE coupling with redshift and/or for different coupling normalization. The case $\epsilon = 0$ corresponds to redshift independent coupling intensity. The case $\epsilon = -1$ with $\beta = 0.244$ correspond to a coupling $C = 1/\phi$. Besides of the different slopes, notice the dependence on the model of the bending scale and, in particular, its dependence on the coupling strength, also in constant coupling models (dash-dotted lines).

Spectra with ordinary downward bending fit both deep sample and CMB data with $n \simeq 1$. Accordingly, low n 's with standard σ_8 's, in general, will cause greater C_ℓ still in the Sachs & Wolfe plateau, while reducing the relative height of the first C_ℓ peak. These effects could be partially compensated by an adjustment of other model parameters, whose search is out of the scopes of this work. Finding n values below 0.7–0.8, however, clearly means that we are dealing with unlikely physical frameworks.

In the case $\epsilon \neq 0$, the discrepancy from unity of the spectral index n , assumed to be constant, is mostly a measure of the distortion caused by the suppression of Meszaros effect, which overwhelms the effects of the displacement of k_{eq} , already considered in

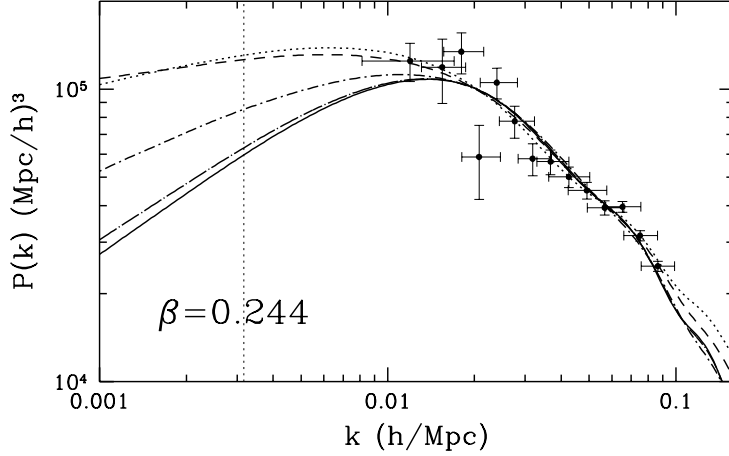


Figure 8. Model comparison with SLOAN digital survey data. Different curves refer to different values of ϵ (as in previous Figure) with the solid line ($\epsilon = 1$) essentially coinciding with an uncoupled model. Constant coupling models ($\epsilon = 0$) are described by dot-dashed curves. Negative ϵ 's yield a further decrease of n . The vertical dotted line is the approximate scale where the Sachs & Wolfe C_l plateau begins. Constant coupling causes a rise of C_{10} by a factor ~ 1.8 . A further factor ~ 2 arises from a coupling $C = 1/\phi$.

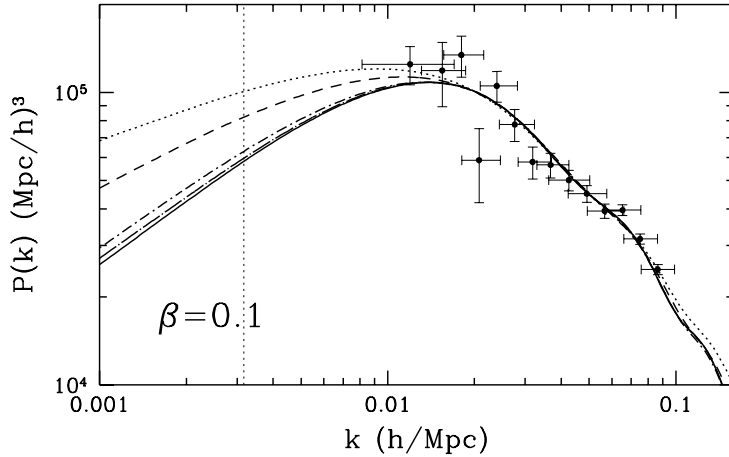


Figure 9. As fig. 8, for a smaller coupling intensity. The effect on the C_{10} scale is much reduced, for constant coupling; however, variable coupling yields a dramatic decrease of n and, for $\epsilon = -1$, the level of $\beta = 0.244$ is almost attained.

the $\beta = \text{const.}$ case. Moreover, such discrepancy is a significant estimate of the distance of the model from uncoupled DE physics. Our fits, shown in Figures 8 and 9, are complemented by 1- and 2- σ intervals around best-fit n values (Figure 10); they are an indication of which models, by adjusting other parameters, might be susceptible to approach the observational scenario. The behavior of transferred spectra in respect to data, when taking n values at 1- and 2- σ from best fits is also shown in Figure 11 (similar to Fig. 3).

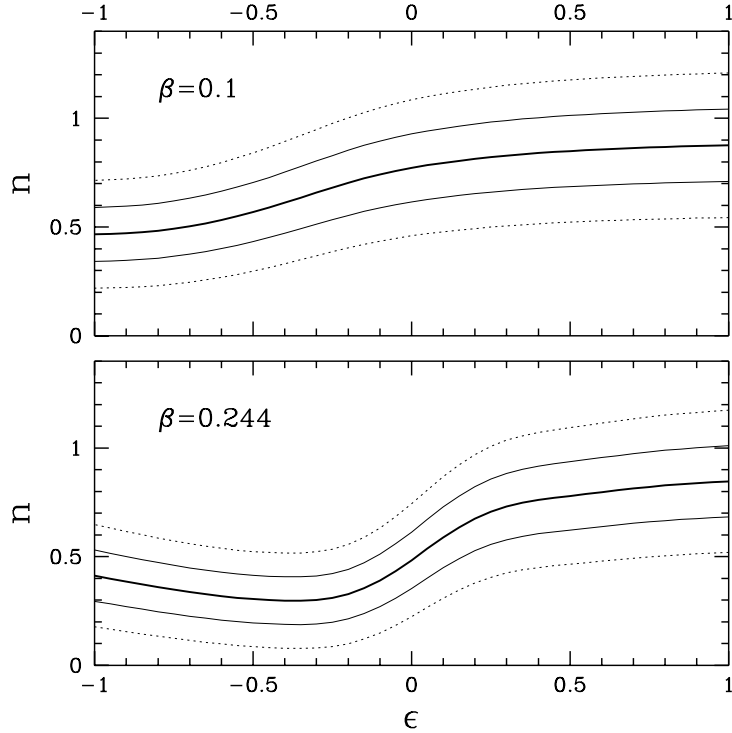


Figure 10. 1– and 2– σ intervals of n , when ϵ varies, for β values.

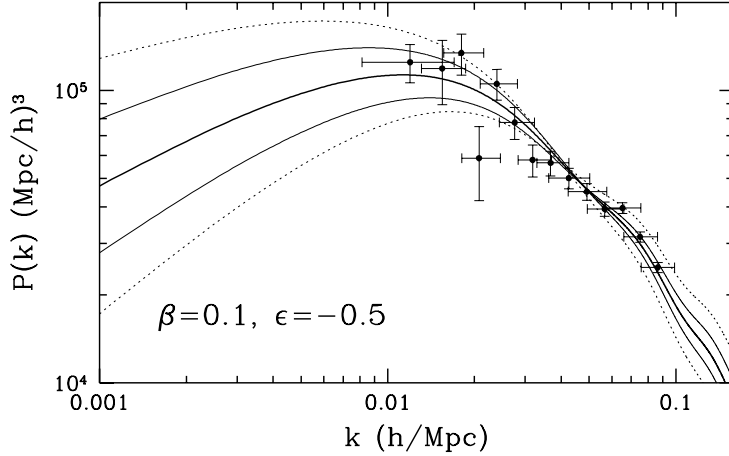


Figure 11. If values of n at 1– or 2– σ ’s from best fits are taken, spectra are significantly modified. Here we show the effect in the case with $C = 0.4(\pi/3)^{1/2}/\sqrt{m_p\phi}$.

If we take $n = 0.75$ at $1-\sigma$ as a threshold to discard a model, no $\epsilon < 0$ coupled model is allowed with $\beta = 0.244$, while $\beta < -0.5$ are also inhibited with $\beta = 0.1$. At $2-\sigma$'s the situation is not much improved for $\beta = 0.244$, while lower values of ϵ are admitted for $\beta = 0.1$. In particular, a model with $C = 1/\phi$, as the *dual-axion* model, lays outside of the range indicated.

The analysis was extended here to models with positive ϵ , for which coupling rises while ϕ increases. A large deal of these models is apparently allowed.

5. Conclusions

The quest for models fitting observational data and avoiding fine tuning and coincidence suggests to test cosmologies where DM is coupled to dynamical DE. It is then important to recognize that quite a few models, with constant or variable DM–DE coupling, are consistent with observational data, although their likelihood might be slightly smaller than uncoupled models.

An important issue, within this context, is finding a way to represent the expected discrepancy of a new cosmology from standard best-fitting models, aiming to transparent results able to avoid a massive use of numerically expensive techniques, as those testing model likelihood in detail; furthermore, the interpretation of likelihood plots is often uneasy, also owing to the large sets of parameters to be disentangled. As far as coupled DE models are concerned, we find that their general feature, when fitted to deep galaxy sample data, is to require a primeval spectral index n significantly below unity. This is true for constant DM–DE coupling and, as we showed here, even truer when the coupling $C \propto \phi^\epsilon$, with negative ϵ . In fact, in this latter case, we showed that the main problems arise from a partial or total suppression of the Meszaros effect, so that the bending of the transfer function $\mathcal{T}(k)$, at $k > k_{eq}$, is softened.

Requiring a value of $n \sim \mathcal{O}(0.6)$ is not a conceptual inconsistency; *e.g.*, inflationary models providing lower n values can be devised; we expect, instead, a conflict with CMB data, which provide us information on model behavior before the onset of any kind of non-linearity, unless the primeval spectrum bends, in the suitable scale range, to compensate the shallower transfer function.

Such a feature, although *ad-hoc* and unlikely, cannot be excluded a priori. However, in this paper, we used the discrepancy of (constant) n from unity as an indicator of model reliability. Together with best-fitting n values we provided also the $1-$ and $2-\sigma$ range of admitted n 's, so that we can evaluate how far from best-fit we can go, to meet other data, without expecting a dramatic drop of model likelihood.

Admittedly, within the present observational framework, there lacks any specific phenomenological push to invoking a DM–DE coupling. Yet, best fitting models, even apart of their conceptual weakness, cause a number of questionable predictions, *e.g.* NFW profiles. Interactions within the dark side were often advocated to cure such difficulties.

Furthermore, fresh data on the redshift dependence of ρ_c , ρ_b and ρ_{DE} , at $z \sim 1\text{--}5$,

might soon be available, if experiments like DUNE [18] will become operational. The discovery of an anomalous scaling of ρ_c , for instance, would set a strong prior, completely biasing likelihood distributions, just as priors on the value of h (Hubble parameter) suppress the likelihood of SCDM models with $h \sim 0.4$, which would otherwise allow a reasonable fit of large sets of data [19]. In particular, models with rising coupling ($\epsilon > 0$) could become an important option. Such coupling behavior, apart of being possibly related to specific particle physics, could also be thought as a phenomenological description of more complex underlying physics, through a DE model.

Acknowledgments

Luca Amendola and Loris Colombo are gratefully thanked for their comments on this work.

References

- [1] Wetterich C. 1988, Nucl.Phys.B 302, 668; Ratra B. & Peebles P.J.E., 1988, Phys.Rev.D 37, 3406
- [2] Peebles P.J.E. & Ratra B., 2003, Rev.Mod.Phys. 75, 559
- [3] Kolb E.W., Matarrese S. & Riotto A., 2006, New J.Phys. 8, 322
- [4] Ellis J., Kalara S., Olive K.A. & Wetterich C., 1989, Phys. Lett. B228, 264; Wetterich C., 1995, A&A 301, 321 Amendola L., 2000, Phys.Rev. D62, 043511 Gasperini M., Piazza F. & Veneziano G., 2002, Phys.Rev. D65, 023508
- [5] Casas J.A., Garca-Bellido J & Quiros M., 1992, Class.Quant.Grav. 9, 1371; Anderson & Carroll, Procs. of “COSMO-97, First International Workshop on Particle Physics and the Early Universe”, Ambleside, England, September 15-19, 1997, astro-ph/9711288; Bartolo N. & Pietroni M., 2000, Phys.Rev. D61, 023518; Pietroni M., 2003, Phys.Rev D67, 103523; Chimento L.P., Jakubi A.S., Pavon D. & Zimdahl W., 2003, Phys.Rev D67, 083513; Rhodes C.S., van de Bruck C., Brax P., & Davis A.C., 2003, Phys.Rev. D68, 083511; Farrar G.R. & Peebles P.J.E., 2004, ApJ 604, 1 Gromov A., Baryshev Y. & Teerikorpi P., 2004, A&A, 415, 813
- [6] Mainini R. & Bonometto S.A., 2004, Phys.Rev.Lett. 93, 121301
- [7] Peccei R.D. & Quinn H.R. 1977, Phys.Rev.Lett. 38, 1440; Weinberg S. 1978, Phys.Rev.Lett. 40, 223; Wilczek F. 1978, Phys.Rev.Lett. 40, 279; Kim J.E. 1979, Phys.Rev.Lett. 43, 103
- [8] Preskill J. et al 1983, Phys.Lett B120, 225; Abbott L. & Sikivie P. 1983 Phys.Lett B120, 133; Dine M. & Fischler 1983 Phys.Lett B120, 137; Turner M.S. 1986 Phys.Rev.D 33, 889
- [9] Mainini R., Colombo L. & Bonometto S.A., 2005, ApJ 632, 691
- [10] Spergel D.N. et al. 2006, ApJ (in press), astro-ph/0603449
- [11] Brax P. & Martin J., 1999, Phys.Lett., B468, 40; Brax P. & Martin J., 2001, Phys.Rev. D61, 10350; Brax P., Martin J., Riazuelo A., 2000, Phys.Rev. D62, 103505
- [12] Colombo L.P.L. & Gervasi M., 2006, JCAP 0610, 001
- [13] Coles M. & Lucchin, 1995, Cosmology, John Wiley & Sons, Chichester
- [14] Amendola L. & Quercellini C., 2003, Phys. Rev. D69; Maccio’ A. V., Quercellini C., Mainini R., Amendola L., Bonometto S. A., 2004, Phys. Rev. D69, 123516
- [15] Lee S., Liu G. & Ng K., 2006, Phys.Rev. D73, 083516; Guo Z., Ohta N. & Tsujikawa S., 2007, astro-ph/0702015
- [16] Tegmark M. et al., 2006, Phys.Rev. D74, 123507
- [17] Amendola L., 2004, Phys.Rev.D69, 103524
- [18] Réfrégier A. et al., Procs. of SPIE symposium ”Astronomical Telescopes and Instrumentation”, Orlando, may 2006, astro-ph/0610062

[19] Blanchard A., Douspis M., Sarkar S., Rowan-Robinson M., 2003, A&A 412, 35